

VLA AND XMM-NEWTON OBSERVATIONS OF SNR W41/TEV γ -RAY SOURCE HESS J1834-087

W.W. TIAN^{1,2}, Z. LI³, D.A. LEAHY², Q.D. WANG³

Draft version May 26, 2019

ABSTRACT

The recently discovered extended TeV source HESS J1834-087 is associated with both a diffuse X-ray enhancement and a molecular cloud, projected at the center of an old radio supernova remnant G23.3-0.3 (SNR W41). New HI observations from the VLA Galactic Plane Survey (VGPS) show unambiguous structures associated with W41 in the radial velocity range of 53 to 63 km/s, so we obtain W41 distance of about 4 ± 0.2 kpc. A new higher sensitivity VGPS continuum image of W41 at 1420 MHz shows faint emission in its eastern part not detected by previous observations, so we give a new angular size of $36' \times 30'$ in b - l direction (average radius of 19 pc). We estimate for W41 a Sedov age of $\sim 8 \times 10^4$ yr. New XMM-Newton observation reveals diffuse X-ray emission within the HESS source and suggests an association between the X-ray and γ -ray emission. The high-resolution ^{13}CO images of W41 further reveal a giant molecular cloud (GMC) located at the center of W41, likely associated with W41 in the the radial velocity range of 61 to 66 km/s. These give first observational evidence that an old SNR encounters a GMC to emit TeV γ -rays in the GMC.

Subject headings: supernova remnants:individual (W41)- γ -rays:individual (HESS J1834-087)

1. INTRODUCTION

Young supernova remnants (SNRs) are one of the main galactic populations to generate very high energy (VHE, above 10^{11} eV) γ -rays (Torres et al. 2003). Observationally, TeV γ -rays have been detected from the Crab Nebula (i.e., SN1054, Weekes et al. 1989), the SNRs RX J1713.7-3946 (i.e., G347.3-0.5, Enomoto et al. 2002) and RX J0852.0-4622 (i.e., G266.2-1.2, Aharonian et al. 2005a). Theoretically, acceleration mechanisms for relativistic electrons at SNR shock fronts have been well-established (Malkov & Drury 2001). Recently, Aharonian et al.'s (2006) survey of the inner part of our Galaxy has revealed 14 new TeV γ -ray sources. The origins of some of them remain uncertain. Yamazaki et al. (2006) showed that TeV γ -rays can originate from an old SNR of an age around 10^5 yr or from a giant molecular cloud (GMC) encountered by the SNR, via pion decay from proton-proton collision. In their scenario, the flux ratio of the γ -rays to the associated X-ray emission is much higher than that from a young SNR. In this letter, we give first observational evidence that an old SNR encounters a GMC to emit TeV γ -rays, based on new radio and X-ray observations as well as recent ^{13}CO images of SNR W41, which is spatially coincident with HESS J1834-087, one of the 14 TeV sources.

2. RADIO AND X-RAY OBSERVATIONS

The radio continuum and HI emission data sets come from the VLA Galactic Plane Survey (VGPS) which is described in detail by Stil et al. (2006). The data sets are mainly based on observations from VLA of the National Radio Astronomy Observatory (NRAO). The spatial resolution of the continuum images of W41 is $1'$ (FWHM)

at 1420 MHz. The synthesized beam for the HI line images is $1'$ and the radial velocity resolution is 1.56 km/s. The short-spacing information for the H I spectral line images is from additional observations with the 100 m Green Bank Telescope of the NRAO.

SNR W41 was observed by XMM-Newton on September 18, 2005 (Obs. ID 0302560301; PI: G. Pühlhofer), with a 20 ksec exposure. In this work, we only used data obtained from the EPIC-PN. We used SAS, version 7.0.0, for data reduction. We selected PN events with patterns 0 through 4 and applied flag filter FLAG==0. Excluding time intervals contaminated by background flares results in a net exposure of 12.4 ksec. We then constructed exposure maps in the 0.3-0.7, 0.7-1.5, 1.5-3, and 3-7 keV bands for flat-fielding. We applied the “filter wheel closed” (FWC) data for instrumental background subtraction. We also detected point-like sources using a detection procedure detailed by Wang (2004).

3. RESULTS

3.1. Continuum Emission

The VGPS continuum image of W41 at 1420 MHz is shown in Fig. 1. The VGPS map has a higher resolution (3 times) and sensitivity, and shows much better detail than the previous image at 330 MHz (Kassim 1992). Prominent filament structure outlines W41. Fainter emissions, not detected by previous observations, appear in its eastern part. The new image gives a corrected angular size of W41: $36' \times 30'$ in b - l direction. The HII regions overlapping in W41 have been resolved into at least three components. We have derived integrated flux density 59.7 ± 8.2 Jy of W41 (including HII regions in the SNR) of 1420 MHz. The resulting 330-1420 MHz spectral index (the flux density is 143 ± 29 Jy at 330 MHz including HII regions, Kassim 1992), has a lower limit of 0.60 ± 0.17 . The TeV γ -ray source HESS J1934-087, detected by Aharonian et al. (2005b), is located at the center of W41. Its location and extent is shown by a solid circle (white), centered at $(l, b) = (23.24, -0.32)$ with

¹ National Astronomical Observatories, CAS, Beijing 100012, China; email: tww@iras.ualgary.ca

² Department of Physics & Astronomy, University of Calgary, Calgary, Alberta T2N 1N4, Canada

³ Department of Astronomy, University of Massachusetts, 710 North Pleasant Street, Amherst, MA 01003, USA

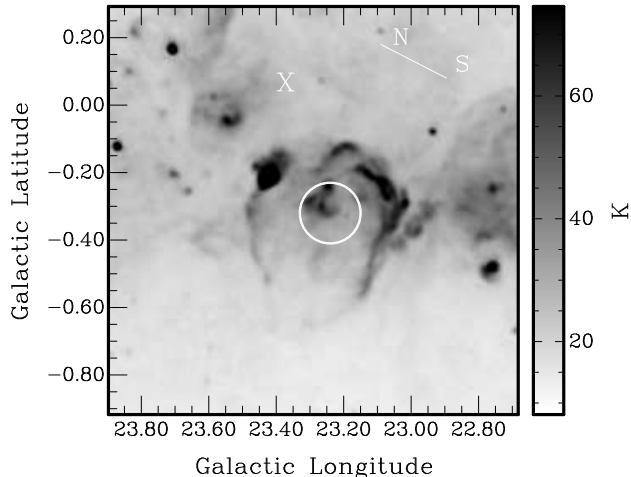


FIG. 1.— The VGPS continuum image of W41 at 1420 MHz. The central circle shows position and extent of the TeV γ -ray HESS J1934-087. The pulsar PSR J1933-0827 is marked by letter X. The direction of North(N) and South(S) is marked.

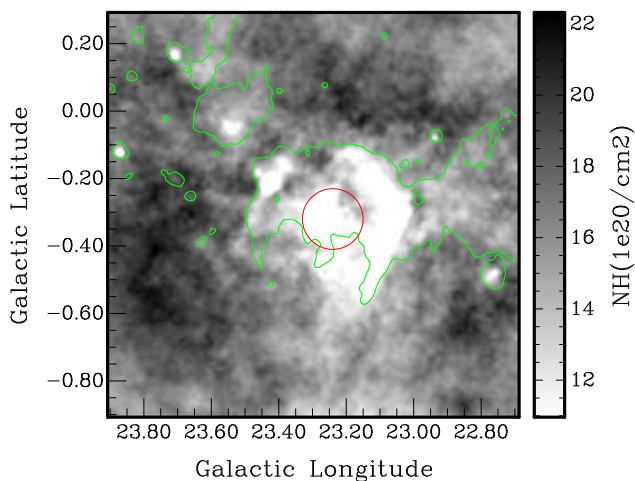


FIG. 2.— The the column density map of the VGPS HI-line emissions associated with W41. This map has superimposed on a W41's contour at 30 K of continuum emission at 1420 MHz chosen to show the SNR (green). The red circle shows the position and extent of HESS J1834-087

a radius of $5\frac{1}{4}$ (Aharonian et al. 2006). The pulsar PSR J1933-0827, which was proposed to associate with W41 by Gaensler and Johnston (1995), is marked by letter X.

3.2. HI and CO Emission

We have searched the VGPS radial velocity range for features in the HI which might relate to the morphology of W41. There are unambiguous HI emissions coincident with the SNR in the velocity range: 53 to 63 km/s. Fig. 2 is the column density map of HI emission integrating over channels from 53 to 63 km/s in units of 10^{20} atom cm^{-2} . The map has superimposed the 30 K contour of 1420 MHz continuum emission chosen to show the SNR. The circle is the same as Fig.1.

We extract ^{13}CO images of W41 from the survey of Jackson et al.(2006). A giant molecular cloud is found at the center of W41 and in the radial velocity range of 61 to 66 km/s so is highly likely associated with W41.

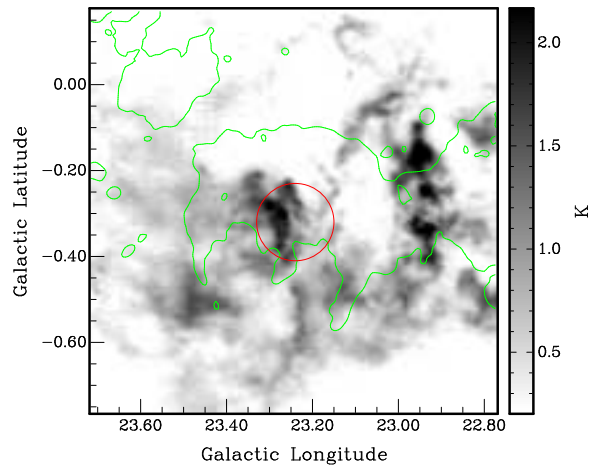


FIG. 3.— The averaged ^{13}CO emission in the field centered on W41 from 61 to 66 km/s. The contour (green) and circle (red) in the map have same meaning as Fig. 2

Fig. 3 shows the averaged ^{13}CO map for channels from 61 to 66 km/s. The contour and circle in the map are the same as in Fig. 2.

3.3. X-ray Emission

The X-ray images of SNR W41 are shown in Fig. 4 for the soft (0.3-1.5 keV) and hard (3-7 keV) bands. In the soft band, the bulk of the field is of smooth, low intensities. In the hard band, a region of enhanced intensities is clearly present within the extent of HESS J1834-087. This feature of enhancement is not related to any detected point-like source, instead, it is apparently diffuse. Given its location, this feature is likely associated with HESS J1834-087.

We perform spectral analysis for the feature, for which we extract a spectrum from a circle centering at $(l, b)=(23.243, -0.331)$ with a radius of $2\frac{1}{5}$ (Fig. 4). To determine the local sky background, we extract a spectrum from a concentric circle with a radius of $7\frac{1}{5}$ and with the enclosed circle representing HESS J1834-087 and detected point-like sources excluded. The two spectra are shown in Fig. 5. Part of the background emission may arise from the interior of the remnant and vary between the source and background regions. Thus our procedure of background determination might be affected by this non-uniformity. Nevertheless, encouraged by the apparently uniform surface intensity at energies below 1.5 keV (Fig. 4), we assume that the background emission also varies little at higher energies. We use the X-ray Spectral Fitting Package (XSPEC) to fit the background spectrum and find that it can be characterized by a combined model consisting of a thermal plasma component (APEC in XSPEC) and a power-law component, both subject to absorption (Table 1). These two components, scaled accordingly to the sky area, are applied to account for the background contribution in the source spectrum. The remaining emission in the source spectrum, presumably intrinsic to the feature, is then characterized by an additional component, for which we find a heavily absorbed power-law. Fitting results are listed in Table 1.

4. DISCUSSION AND CONCLUSION

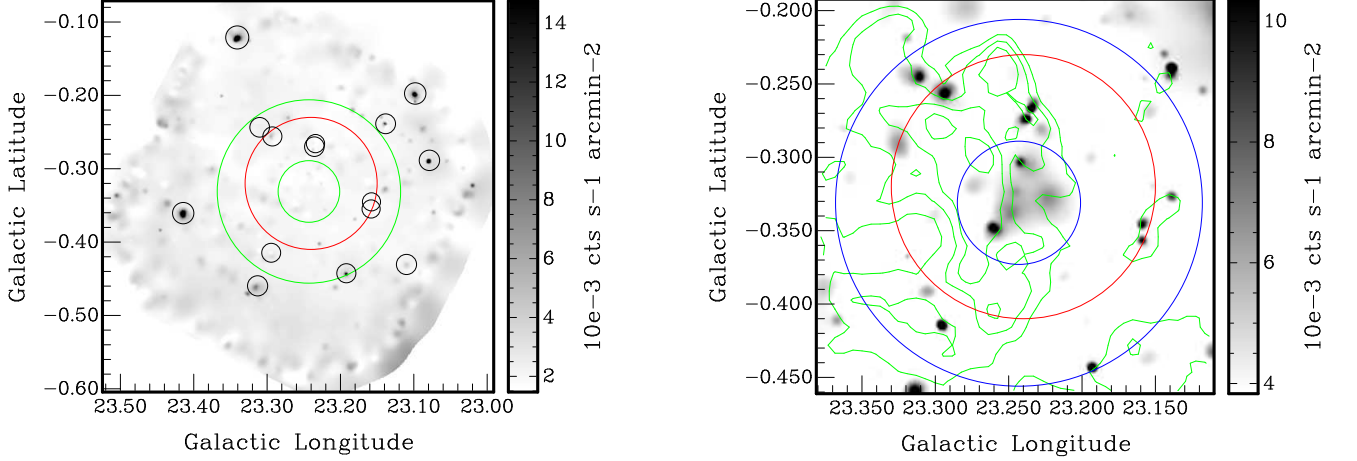


FIG. 4.— XMM-Newton EPIC-PN intensity images of SNR W41 in the 0.3-1.5 (left) and 1.5-7 keV (right) bands. The intensity is adaptively smoothed using *csmooth* to achieve a signal-to-noise ratio of ~ 3 . The middle solid circle (red) represents the location and extent of the γ -ray source HESS J1834-087. The small circle (blue) illustrates the region of spectral interest, while the large circle (blue) outlines the region (with the enclosed middle circle excluded) where the background spectrum is extracted. The smaller solid circles (grey in the left plot) outline detected sources and their extent according to twice the 50% encircled energy radius, which are excluded from spectral extraction. The right plot has superimposed on contours of ^{13}CO emissions from Fig. 3, at 0.8, 1.2, 1.6 and 2.1 k

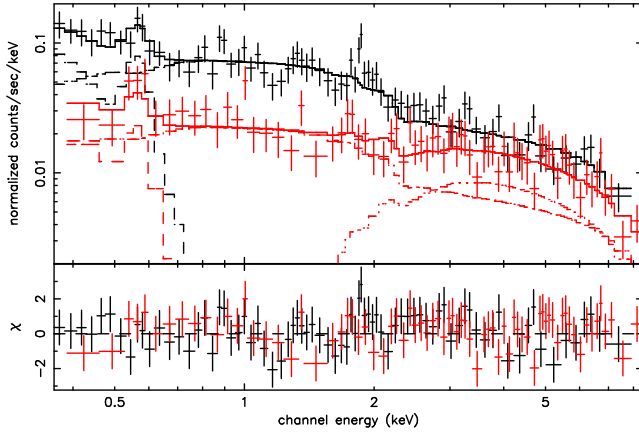


FIG. 5.— EPIC-PN spectra from the SNR W41 region. Red: the spectrum of the X-ray feature associated with HESS J1834-087; Black: the spectrum of local sky background. The spectra are instrumental background-subtracted and are binned to achieve a signal-to-noise ratio better than 3. Also shown are the best-fit models (solid curves) to the spectra and the different model components (dashed and dotted curves). See text for details

4.1. Distance and Age of W41

Using flat galactic rotation velocity $V_R = V_0 = 200$ km/s and $R_0 = 8.0$ kpc, we obtain the SNR's distance of 4 ± 0.2 kpc or 10.7 ± 0.2 kpc. W41 has new averaged angular diameter $33'$, so yields radius about 19 pc ($d=4$ kpc) or 51 pc ($d=10.7$ kpc) for the SNR. Since known shell-type supernova remnants are a few to ~ 20 pc on radius, we use the closer distance. From the HI column density map associated with W41 (Fig. 2), we estimate a N_H of about $5 - 10 \times 10^{20} \text{ cm}^{-2}$, so the density $n_0 = N_H / (2R)$ around W41 is about 6 cm^{-3} . Applying a Sedov model (Cox, 1972), for a typical explosion energy of $E = 0.5 \times 10^{51}$ erg, yields an age of $\sim 8 \times 10^4$ yr.

4.2. X-ray, TeV γ -ray and CO Emission from W41

Previous ^{12}CO observations have shown that W41 was associated with a very large molecular complex (Dame

TABLE 1
FIT TO THE X-RAY SPECTRUM^a

Parameter	Value
$\chi^2/d.o.f.$	61.3/74
$N_{H,1}$ (10^{20} cm^{-2})	3.0 (<9.0) ^b
Temperature (keV; APEC)	$0.09^{+0.03}_{-0.02}$
Photon index (PL1)	$0.80^{+0.13}_{-0.11}$
$N_{H,2}$ (10^{22} cm^{-2})	$6.2^{+3.1}_{-2.5}$
Photon index (PL2)	$2.0^{+0.7}_{-0.8}$
Flux ($10^{-13} \text{ ergs s}^{-1} \text{ cm}^{-2}$) ^c	7.0

REFERENCES. — ^aAn combined model of absorbed ($N_{H,1}$) APEC+power-law (PL1) is used for characterizing the sky background and a second absorbed ($N_{H,1}$) power-law (PL2) is used to model to the emission from the feature; ^bQuoted uncertainties are at 90% confidence level; ^c2-10 keV intrinsic flux for PL2.

et al. 1986). Albert et al. (2006) studied the ^{12}CO images from Dame et al (2001) and suggested the giant molecular cloud associated with W41 is best defined by integrated the ^{12}CO peak emission from 70 to 85 km/s. They also used the ^{13}CO images from Jackson et al. (2006) and confirmed that the recently discovered TeV source HESS J1834-087 lies towards a GMC. However, our observations show the HI-line emissions are associated with W41 in the velocity range of 53 to 63 km/s. ^{13}CO is useful as optically thin tracer of the molecular cloud so we reanalyzed the ^{13}CO images of W41. We found a GMC located at the center of W41 in the radial velocity range of 61 to 66 km/s. Fig. 3 shows the bright ^{13}CO emission in the velocity range and that it is coincident with HESS J1834-087. The X-ray emission (the right plot of Fig. 4) is at the right side of the molecular cloud but still within the molecular cloud. The offset may be due to the left side of the cloud extending be-

hind W41 by more than 1 proton gyroradius, then only the right side is illuminated by the protons. The total H_2 mass of the CO emission peak (over $0.1^\circ \times 0.2^\circ$ region) is estimated from $M_{H_2} = N_{H_2} \Omega d^2 (2m_H/M_\odot)$. We take $N_{H_2}/W_{CO} \approx 1.8 \times 10^{20} \text{ cm}^{-2} \text{ K}^{-1} \text{ km}^{-1} \text{ s}$ from Dame et al. (2001). Total integrated intensity of ^{13}CO is $W_{CO} \approx 5 \text{ K km/s}$ from Fig. 3. Assuming $^{12}\text{CO}/^{13}\text{CO}$ isotopic abundance ratio of 30 (Langer & Penzias 1990), we obtain average H_2 column density of $N_{H_2} \approx 2.7 \times 10^{22} \text{ cm}^{-2}$, and molecular cloud mass of $M_{H_2} \approx 4.5 \times 10^4 M_\odot$. This is a giant molecular cloud with a density of $\sim 10^3 \text{ cm}^{-3}$.

From the observed γ -ray luminosity (Albert et al. 2006), using equation 16 in Torres et al. (2003) and a supernova power of 10^{51} ergs, we obtain a relation between an acceleration efficiency θ of hadrons and the required density n of matter in the γ -ray production region for hadron to be responsible for the observed radiation: $\theta \sim 10^{-2}$ requires $n \sim 10^2 \text{ cm}^{-3}$; $\theta \sim 10^{-3}$ requires $n \sim 10^3 \text{ cm}^{-3}$. Generally, the maximum acceleration efficiency θ of 10% is accepted, so the GMC is dense enough to produce the observed TeV intensity with a lower acceleration efficiency. The protons penetrate deeply into the cloud, only limited by proton gyroradius (which is determined by B in the molecular cloud), not p-p collision cross-section. This could result in the observed offset of peak CO and p-p to π^0 decay TeV γ -rays. The physical peak of X-ray and TeV should be coincident. The column density of the molecular cloud is enough to absorb X-rays and cause offset to the right of observed X-ray peak emission from that true peak and peak of TeV γ -rays.

HESS J1834-087 has an extended nature as revealed by the MAGIC and HESS observations (Albert et al. 2006; Aharonian et al. 2006). From the Swift/X-Ray Telescope (XRT) observations of W41, Landi et al. (2006) found a faint X-ray source within the extent of HESS J1834-087 and thereby suggested a possible pulsar wind nebula (PWN) association. This X-ray source, located at $(l, b) = (23.2340, -0.2657)$, is also detected by the present XMM-Newton observation, but there is no evidence for the existence of a PWN. Instead, the prominent diffuse X-ray feature is most likely associated with the TeV γ -ray emission.

Yamazaki et al. (2006) studied the X-ray and γ -ray emission from evolved SNRs with an age of around 10^5 yr and that from a GMC interacting with the SNR. They showed that TeV γ -ray emission can originate from the SNR, or from the SNR shock running into a GMC, or from the GMC illuminated by high energy protons from the SNR shock. These different origins may be distinguished by the X-ray to γ -ray spectra. A simple

diagnostic is the ratio of the γ -ray to the X-ray flux, $R_{TeV/X} = F_\gamma(1 - 10 \text{ TeV})/F_X(2 - 10 \text{ keV})$. According to Yamazaki et al. (2006), for the three cases (in the above mentioned order), the value of $R_{TeV/X}$ is of order $10 - 10^2$, 10 and $> 10^2$, respectively, for their fiducial SNR parameters. For young SNRs found to show gamma-ray emission, $R_{TeV/X}$ is typically below ~ 2 . For HESS J1834-087, the 1-10 TeV γ -ray flux is $\sim 8 \times 10^{-12} \text{ ergs s}^{-1} \text{ cm}^{-2}$, based on the MAGIC observation (Albert et al. 2006). Our 2-10 keV X-ray flux is $\sim 7 \times 10^{-13} \text{ ergs s}^{-1} \text{ cm}^{-2}$ giving $R_{TeV/X} \simeq 11$, with uncertainty of a factor of two. HESS J1834-087 is possibly arising from a shocked GMC. This is supported by the presence of the GMC as found from the ^{13}CO detection. The velocities indicate that the GMC is just behind W41. The absorption column density of a few 10^{22} cm^{-2} estimated from the X-ray spectral fit (Table 1) also implies that the nonthermal X-ray emission associated with HESS J1834-087 arises from within the GMC and is behind W41. According to Yamazaki et al. (2006), the X-ray emission from a shocked GMC or a GMC illuminated by high energy protons is likely synchrotron emission from secondary electrons arising from hadronic processes. The hard X-ray spectrum that we find is also consistent with such a scenario.

4.3. W41, PSR J1833-0827 and HESS J1834-087

Pulsar J1833-0827 ($b=23.386^\circ$, $l=0.063^\circ$) lies at the north side and about $10'$ away from edge of W41. It has a kinematic distance of 4-5 kpc by HI absorption (Weisberg et al. 1995) and a DM distance of 5.7 kpc and a characteristic age of 147 kyr (Taylor et al. 1993). Our results for distance (4 kpc) and age ($\sim 10^5$ yrs) of W41 are consistent with the pulsar J1833-0827, and support the possible associations W41/PSR J1833-0827 also. However, the pulsar is about $20'$ away from the extended γ -ray source and is not associated with HESS J1834-087.

TWW and LDA acknowledge support from the Natural Sciences and Engineering Research Council of Canada. The research at UMass is supported by the NASA/CXC under the grant GO5-6057X. TWW thanks support from the Natural Science Foundation of China. We thank Dr. Stil for providing the VGPS data. This publication makes use of molecular line data from the Boston University-FCRAO Galactic Ring Survey (GRS). The NRAO is a facility of the National Science Foundation operated under cooperative agreement by Associated Universities, Inc.

REFERENCES

- Aharonian, F., Akhperjanian, A.G., Bazer-Bachi, A.R. et al., 2006, *ApJ*, 636, 777
 Aharonian, F., Akhperjanian, A.G., Bazer-Bachi, A.R. et al. 2005a, *A&A*, 437, L7
 Aharonian, F., Akhperjanian, A.G., Aye, K.-M. et al. 2005b, *Science*, 307, 1938
 Albert, J., Aliu, E., Anderhub, H. et al. 2006, *ApJ*, 643, L53
 Cox, D., 1972, *ApJ*, 178, 159
 Dame, T.M., Hartmann, D., Thaddeus, P., 2001, *ApJ*, 547, 792
 Dame, T.M., Elmegreen, B.G., Cohen, R.S. et al., 1986, *ApJ*, 305, 892
 Enomoto R., Tanimori, T., Naito, T. 2002, *Nature*, 416, 823 2004, *MNRAS*, 353, 1311
 Landi, R., Bassani, L., Malizia, A., 2006, *ApJ*, 651, 190
 Langer, W.D., Penzias, A.A., 1990, *ApJ*, 357, 477
 Gaensler B.M. & Johnston, S., 1995, *MNRAS*, 275, 73
 Kassim, N.E., 1992, *AJ*, 103, 943
 Jackson, J.M., Rathborne, J.M., Shah, R.H. et al. 2006, *ApJ Suppl.*, 163, 145
 Malkov E., Drury L.O'C., 2001, *Rep. Prog. Phys.*, 64, 429
 Taylor, J.H., Manchester, R.N. & Lyne, A.G., 1993, *ApJS*, 88, 529.
 Torres, D.F., Romero, G.E., Dame, T.M. et al. 2003, *Phy. Reports*, 382, 303
 Stil, J.M., Taylor, A.R., Dickey, J.M. et al. 2006, *AJ*, 132, 1158
 Wang Q.D., 2004, *ApJ*, 612, 159
 Weekes, T.C., Cawley, M.F., Fegan, D.J. et al., 1989, *ApJ*, 342, 379
 Weisberg J.M., Siegel, M.H., Frail, D.A. et al., 1995, 447, 204
 Yamazaki, R., Kohri, K., Bamba, A. et al. 2006, *MNRAS*, 371, 1975

VLA AND XMM-NEWTON OBSERVATIONS OF SNR W41/TEV γ -RAY SOURCE HESS J1834-087

W.W. TIAN^{1,2}, Z. LI³, D.A. LEAHY², Q.D. WANG³

Draft version December 11, 2006

ABSTRACT

The recently discovered extended TeV source HESS J1834-087 is associated with both a diffuse X-ray enhancement and a molecular cloud, projected at the center of an old radio supernova remnant G23.3-0.3 (SNR W41). New HI observations from the VLA Galactic Plane Survey (VGPS) show unambiguous structures associated with W41 in the radial velocity range of 53 to 63 km/s, so we obtain W41 distance of about 4 ± 0.2 kpc. A new higher sensitivity VGPS continuum image of W41 at 1420 MHz shows faint emission in its eastern part not detected by previous observations, so we give a new angular size of $36' \times 30'$ in b - l direction (average radius of 19 pc). We estimate for W41 a Sedov age of $\sim 8 \times 10^4$ yr. New XMM-Newton observation reveals diffuse X-ray emission within the HESS source and suggests an association between the X-ray and γ -ray emission. The high-resolution ^{13}CO images of W41 further reveal a giant molecular cloud (GMC) located at the center of W41, likely associated with W41 in the the radial velocity range of 61 to 66 km/s. These give first observational evidence that an old SNR encounters a GMC to emit TeV γ -rays in the GMC.

Subject headings: supernova remnants:individual (W41)- γ -rays:individual (HESS J1834-087)

1. INTRODUCTION

Young supernova remnants (SNRs) are one of the main galactic populations to generate very high energy (VHE, above 10^{11} eV) γ -rays (Torres et al. 2003). Observationally, TeV γ -rays have been detected from the Crab Nebula (i.e., SN1054, Weekes et al. 1989), the SNRs RX J1713.7-3946 (i.e., G347.3-0.5, Enomoto et al. 2002) and RX J0852.0-4622 (i.e., G266.2-1.2, Aharonian et al. 2005a). Theoretically, acceleration mechanisms for relativistic electrons at SNR shock fronts have been well-established (Malkov & Drury 2001). Recently, Aharonian et al.'s (2006) survey of the inner part of our Galaxy has revealed 14 new TeV γ -ray sources. The origins of some of them remain uncertain. Yamazaki et al. (2006) showed that TeV γ -rays can originate from an old SNR of an age around 10^5 yr or from a giant molecular cloud (GMC) encountered by the SNR, via pion decay from proton-proton collision. In their scenario, the flux ratio of the γ -rays to the associated X-ray emission is much higher than that from a young SNR. In this letter, we give first observational evidence that an old SNR encounters a GMC to emit TeV γ -rays, based on new radio and X-ray observations as well as recent ^{13}CO images of SNR W41, which is spatially coincident with HESS J1834-087, one of the 14 TeV sources.

2. RADIO AND X-RAY OBSERVATIONS

The radio continuum and HI emission data sets come from the VLA Galactic Plane Survey (VGPS) which is described in detail by Stil et al. (2006). The data sets are mainly based on observations from VLA of the National Radio Astronomy Observatory (NRAO). The spatial resolution of the continuum images of W41 is $1'$ (FWHM)

at 1420 MHz. The synthesized beam for the HI line images is $1'$ and the radial velocity resolution is 1.56 km/s. The short-spacing information for the H I spectral line images is from additional observations with the 100 m Green Bank Telescope of the NRAO.

SNR W41 was observed by XMM-Newton on September 18, 2005 (Obs. ID 0302560301; PI: G. Puehlhofer), with a 20 ksec exposure. In this work, we only used data obtained from the EPIC-PN. We used SAS, version 7.0.0, for data reduction. We selected PN events with patterns 0 through 4 and applied flag filter FLAG==0. Excluding time intervals contaminated by background flares results in a net exposure of 12.4 ksec. We then constructed exposure maps in the 0.3-0.7, 0.7-1.5, 1.5-3, and 3-7 keV bands for flat-fielding. We applied the “filter wheel closed” (FWC) data for instrumental background subtraction. We also detected point-like sources using a detection procedure detailed by Wang (2004).

3. RESULTS

3.1. Continuum Emission

The VGPS continuum image of W41 at 1420 MHz is shown in Fig. 1. The VGPS map has a higher resolution (3 times) and sensitivity, and shows much better detail than the previous image at 330 MHz (Kassim 1992). Prominent filament structure outlines W41. Fainter emissions, not detected by previous observations, appear in its eastern part. The new image gives a corrected angular size of W41: $36' \times 30'$ in b - l direction. The HII regions overlapping in W41 have been resolved into at least three components. We have derived integrated flux density 59.7 ± 8.2 Jy of W41 (including HII regions in the SNR) of 1420 MHz. The resulting 330-1420 MHz spectral index (the flux density is 143 ± 29 Jy at 330 MHz including HII regions, Kassim 1992), has a lower limit of 0.60 ± 0.17 . The TeV γ -ray source HESS J1934-087, detected by Aharonian et al.(2005b), is located at the center of W41. Its location and extent is shown by a solid circle (white), centered at $(l, b) = (23.24, -0.32)$ with

¹ National Astronomical Observatories, CAS, Beijing 100012, China; email: tww@irao.ucas.ac.cn

² Department of Physics & Astronomy, University of Calgary, Calgary, Alberta T2N 1N4, Canada

³ Department of Astronomy, University of Massachusetts, 710 North Pleasant Street, Amherst, MA 01003, USA

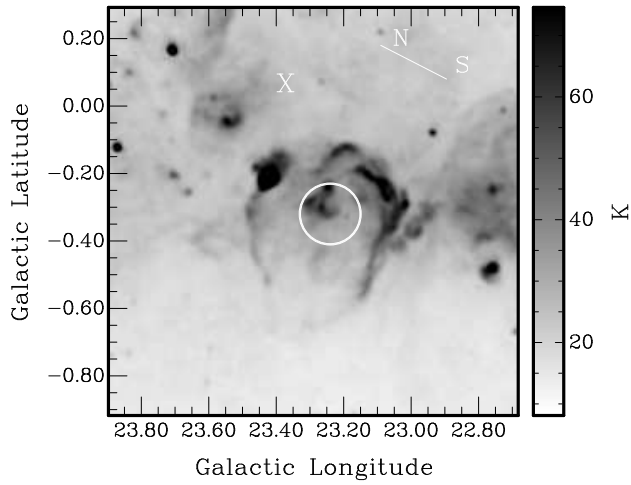


FIG. 1.— The VGPS continuum image of W41 at 1420 MHz. The central circle shows position and extent of the TeV γ -ray HESS J1934-087. The pulsar PSR J1933-0827 is marked by letter X. The direction of North(N) and South(S) is marked.

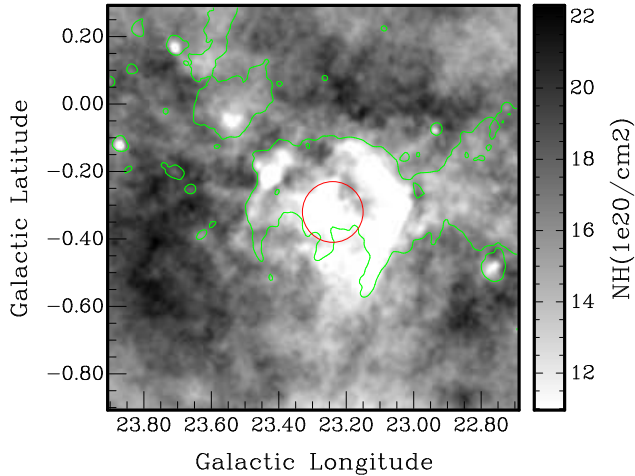


FIG. 2.— The the column density map of the VGPS HI-line emissions associated with W41. This map has superimposed on a W41's contour at 30 K of continuum emission at 1420 MHz chosen to show the SNR (green). The red circle shows the position and extent of HESS J1834-087

a radius of 5.4 (Aharonian et al. 2006). The pulsar PSR J1933-0827, which was proposed to associate with W41 by Gaensler and Johnston (1995), is marked by letter X.

3.2. HI and CO Emission

We have searched the VGPS radial velocity range for features in the HI which might relate to the morphology of W41. There are unambiguous HI emissions coincident with the SNR in the velocity range: 53 to 63 km/s. Fig. 2 is the column density map of HI emission integrating over channels from 53 to 63 km/s in units of 10^{20} atom cm^{-2} . The map has superimposed the 30 K contour of 1420 MHz continuum emission chosen to show the SNR. The circle is the same as Fig.1.

We extract ^{13}CO images of W41 from the survey of Jackson et al.(2006). A giant molecular cloud is found at the center of W41 and in the radial velocity range of 61 to 66 km/s so is highly likely associated with W41.

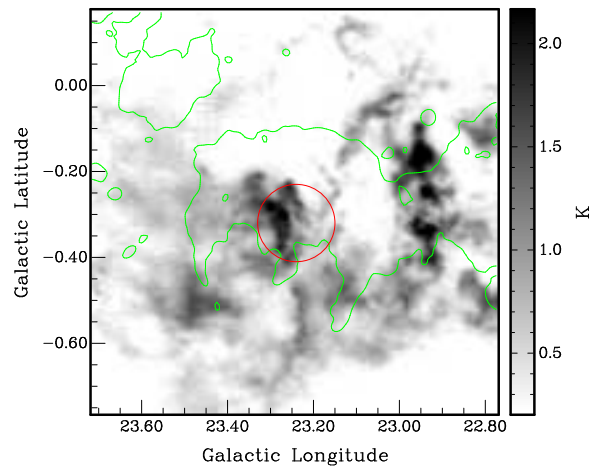


FIG. 3.— The averaged ^{13}CO emission in the field centered on W41 from 61 to 66 km/s. The contour (green) and circle (red) in the map have same meaning as Fig. 2

Fig. 3 shows the averaged ^{13}CO map for channels from 61 to 66 km/s. The contour and circle in the map are the same as in Fig. 2.

3.3. X-ray Emission

The X-ray images of SNR W41 are shown in Fig. 4 for the soft (0.3-1.5 keV) and hard (3-7 keV) bands. In the soft band, the bulk of the field is of smooth, low intensities. In the hard band, a region of enhanced intensities is clearly present within the extent of HESS J1834-087. This feature of enhancement is not related to any detected point-like source, instead, it is apparently diffuse. Given its location, this feature is likely associated with HESS J1834-087.

We perform spectral analysis for the feature, for which we extract a spectrum from a circle centering at $(l, b)=(23.243, -0.331)$ with a radius of 2.5 (Fig. 4). To determine the local sky background, we extract a spectrum from a concentric circle with a radius of 7.5 and with the enclosed circle representing HESS J1834-087 and detected point-like sources excluded. The two spectra are shown in Fig. 5. Part of the background emission may arise from the interior of the remnant and vary between the source and background regions. Thus our procedure of background determination might be affected by this non-uniformity. Nevertheless, encouraged by the apparently uniform surface intensity at energies below 1.5 keV (Fig. 4), we assume that the background emission also varies little at higher energies. We use the X-ray Spectral Fitting Package (XSPEC) to fit the background spectrum and find that it can be characterized by a combined model consisting of a thermal plasma component (APEC in XSPEC) and a power-law component, both subject to absorption (Table 1). These two components, scaled accordingly to the sky area, are applied to account for the background contribution in the source spectrum. The remaining emission in the source spectrum, presumably intrinsic to the feature, is then characterized by an additional component, for which we find a heavily absorbed power-law. Fitting results are listed in Table 1.

4. DISCUSSION AND CONCLUSION

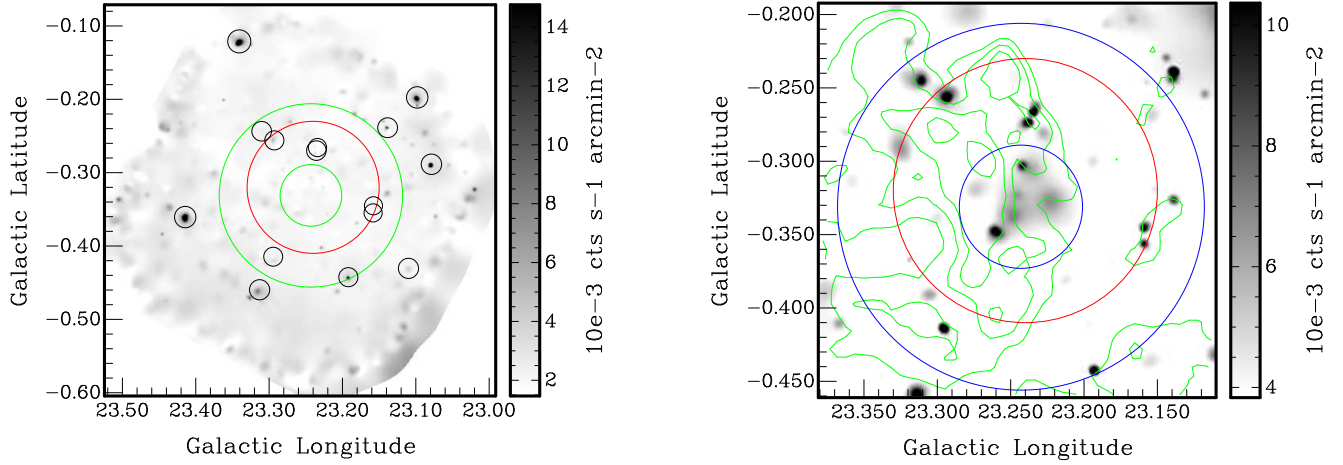


FIG. 4.— XMM-Newton EPIC-PN intensity images of SNR W41 in the 0.3-1.5 (left) and 1.5-7 keV (right) bands. The intensity is adaptively smoothed using *csmooth* to achieve a signal-to-noise ratio of ~ 3 . The middle solid circle (red) represents the location and extent of the γ -ray source HESS J1834-087. The small circle (blue) illustrates the region of spectral interest, while the large circle (blue) outlines the region (with the enclosed middle circle excluded) where the background spectrum is extracted. The smaller solid circles (grey in the left plot) outline detected sources and their extent according to twice the 50% encircled energy radius, which are excluded from spectral extraction. The right plot has superimposed on contours of ^{13}CO emissions from Fig. 3, at 0.8, 1.2, 1.6 and 2.1 k

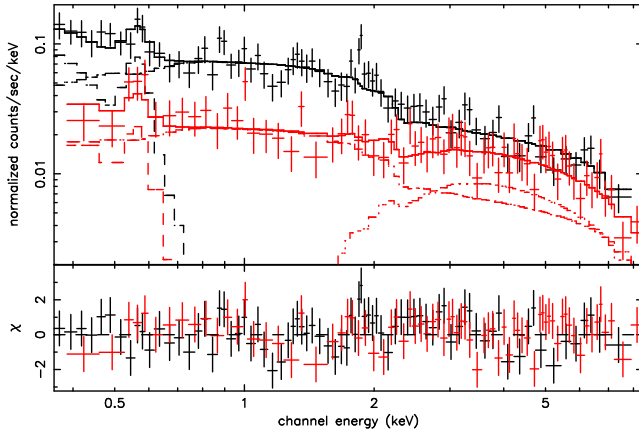


FIG. 5.— EPIC-PN spectra from the SNR W41 region. Red: the spectrum of the X-ray feature associated with HESS J1834-087; Black: the spectrum of local sky background. The spectra are instrumental background-subtracted and are binned to achieve a signal-to-noise ratio better than 3. Also shown are the best-fit models (solid curves) to the spectra and the different model components (dashed and dotted curves). See text for details

4.1. Distance and Age of W41

Using flat galactic rotation velocity $V_R = V_0 = 200$ km/s and $R_0 = 8.0$ kpc, we obtain the SNR's distance of 4 ± 0.2 kpc or 10.7 ± 0.2 kpc. W41 has new averaged angular diameter $33'$, so yields radius about 19 pc ($d = 4$ kpc) or 51 pc ($d = 10.7$ kpc) for the SNR. Since known shell-type supernova remnants are a few to ~ 20 pc on radius, we use the closer distance. From the HI column density map associated with W41 (Fig. 2), we estimate a N_H of about $5 - 10 \times 10^{20} \text{ cm}^{-2}$, so the density $n_0 = N_H / (2R)$ around W41 is about 6 cm^{-3} . Applying a Sedov model (Cox, 1972), for a typical explosion energy of $E = 0.5 \times 10^{51}$ erg, yields an age of $\sim 8 \times 10^4$ yr.

4.2. X-ray, TeV γ -ray and CO Emission from W41

Previous ^{12}CO observations have shown that W41 was associated with a very large molecular complex (Dame

TABLE 1
FIT TO THE X-RAY SPECTRUM^a

Parameter	Value
$\chi^2/d.o.f.$	61.3/74
$N_{H,1}$ (10^{20} cm^{-2})	$3.0 (<9.0)^b$
Temperature (keV; APEC) ..	$0.09^{+0.03}_{-0.02}$
Photon index (PL1)	$0.80^{+0.13}_{-0.11}$
$N_{H,2}$ (10^{22} cm^{-2})	$6.2^{+3.1}_{-2.5}$
Photon index (PL2)	$2.0^{+0.7}_{-0.8}$
Flux ($10^{-13} \text{ ergs s}^{-1} \text{ cm}^{-2}$) ^c	7.0

REFERENCES. — ^aAn combined model of absorbed ($N_{H,1}$) APEC+power-law (PL1) is used for characterizing the sky background and a second absorbed ($N_{H,1}$) power-law (PL2) is used to model to the emission from the feature; ^bQuoted uncertainties are at 90% confidence level; ^c2-10 keV intrinsic flux for PL2.

et al. 1986). Albert et al. (2006) studied the ^{12}CO images from Dame et al (2001) and suggested the giant molecular cloud associated with W41 is best defined by integrated the ^{12}CO peak emission from 70 to 85 km/s. They also used the ^{13}CO images from Jackson et al. (2006) and confirmed that the recently discovered TeV source HESS J1834-087 lies towards a GMC. However, our observations show the HI-line emissions are associated with W41 in the velocity range of 53 to 63 km/s. ^{13}CO is useful as optically thin tracer of the molecular cloud so we reanalyzed the ^{13}CO images of W41. We found a GMC located at the center of W41 in the radial velocity range of 61 to 66 km/s. Fig. 3 shows the bright ^{13}CO emission in the velocity range and that it is coincident with HESS J1834-087. The X-ray emission (the right plot of Fig. 4) is at the right side of the molecular cloud but still within the molecular cloud. The offset may be due to the left side of the cloud extending behind W41 by more than 1 proton gyroradius, then only

the right side is illuminated by the protons. The total H_2 mass of the CO emission peak (over $0.1^\circ \times 0.2^\circ$ region) is estimated from $M_{H_2} = N_{H_2} \Omega d^2 (2m_H / M_\odot)$. We take $N_{H_2} / W_{CO} \approx 1.8 \times 10^{20} \text{ cm}^{-2} \text{ K}^{-1} \text{ km}^{-1} \text{ s}$ from Dame et al. (2001). Total integrated intensity of ^{13}CO is $W_{CO} \approx 5 \text{ K km/s}$ from Fig. 3. Assuming $^{12}\text{CO}/^{13}\text{CO}$ isotopic abundance ratio of 30 (Langer & Penzias 1990), we obtain average H_2 column density of $N_{H_2} \approx 2.7 \times 10^{22} \text{ cm}^{-2}$, and molecular cloud mass of $M_{H_2} \approx 4.5 \times 10^4 M_\odot$. This is a giant molecular cloud with a density of $\sim 10^3 \text{ cm}^{-3}$.

From the observed γ -ray luminosity (Albert et al. 2006), using equation 16 in Torres et al. (2003) and a supernova power of 10^{51} ergs, we obtain a relation between an acceleration efficiency θ of hadrons and the required density n of matter in the γ -ray production region for hadron to be responsible for the observed radiation: $\theta \sim 10^{-2}$ requires $n \sim 10^2 \text{ cm}^{-3}$; $\theta \sim 10^{-3}$ requires $n \sim 10^3 \text{ cm}^{-3}$. Generally, the maximum acceleration efficiency θ of 10% is accepted, so the GMC is dense enough to produce the observed TeV intensity with a lower acceleration efficiency. The protons penetrate deeply into the cloud, only limited by proton gyroradius (which is determined by B in the molecular cloud), not p-p collision cross-section. This could result in the observed offset of peak CO and p-p to π^0 decay TeV γ -rays. The physical peak of X-ray and TeV should be coincident. The column density of the molecular cloud is enough to absorb X-rays and cause offset to the right of observed X-ray peak emission from that true peak and peak of TeV γ -rays.

HESS J1834-087 has an extended nature as revealed by the MAGIC and HESS observations (Albert et al. 2006; Aharonian et al. 2006). From the Swift/X-Ray Telescope (XRT) observations of W41, Landi et al. (2006) found a faint X-ray source within the extent of HESS J1834-087 and thereby suggested a possible pulsar wind nebula (PWN) association. This X-ray source, located at $(l, b) = (23.2340, -0.2657)$, is also detected by the present XMM-Newton observation, but there is no evidence for the existence of a PWN. Instead, the prominent diffuse X-ray feature is most likely associated with the TeV γ -ray emission.

Yamazaki et al. (2006) studied the X-ray and γ -ray emission from evolved SNRs with an age of around 10^5 yr and that from a GMC interacting with the SNR. They showed that TeV γ -ray emission can originate from the SNR, or from the SNR shock running into a GMC, or from the GMC illuminated by high energy protons from the SNR shock. These different origins may be distinguished by the X-ray to γ -ray spectra. A simple diagnostic is the ratio of the γ -ray to the X-ray flux,

$R_{TeV/X} = F_\gamma(1 - 10 \text{ TeV}) / F_X(2 - 10 \text{ keV})$. According to Yamazaki et al. (2006), for the three cases (in the above mentioned order), the value of $R_{TeV/X}$ is of order $10 - 10^2$, 10 and $> 10^2$, respectively, for their fiducial SNR parameters. For young SNRs found to show gamma-ray emission, $R_{TeV/X}$ is typically below ~ 2 . For HESS J1834-087, the 1-10 TeV γ -ray flux is $\sim 8 \times 10^{-12} \text{ ergs s}^{-1} \text{ cm}^{-2}$, based on the MAGIC observation (Albert et al. 2006). Our 2-10 keV X-ray flux is $\sim 7 \times 10^{-13} \text{ ergs s}^{-1} \text{ cm}^{-2}$ giving $R_{TeV/X} \simeq 11$, with uncertainty of a factor of two. HESS J1834-087 is possibly arising from a shocked GMC. This is supported by the presence of the GMC as found from the ^{13}CO detection. The velocities indicate that the GMC is just behind W41. The absorption column density of a few 10^{22} cm^{-2} estimated from the X-ray spectral fit (Table 1) also implies that the nonthermal X-ray emission associated with HESS J1834-087 arises from within the GMC and is behind W41. According to Yamazaki et al. (2006), the X-ray emission from a shocked GMC or a GMC illuminated by high energy protons is likely synchrotron emission from secondary electrons arising from hadronic processes. The hard X-ray spectrum that we find is also consistent with such a scenario.

4.3. W41, PSR J1833-0827 and HESS J1834-087

Pulsar J1833-0827 ($b=23.386^\circ$, $l=0.063^\circ$) lies at the north side and about $10'$ away from edge of W41. It has a kinematic distance of 4-5 kpc by HI absorption (Weisberg et al. 1995) and a DM distance of 5.7 kpc and a characteristic age of 147 kyr (Taylor et al. 1993). Our results for distance (4 kpc) and age ($\sim 10^5$ yrs) of W41 are consistent with the pulsar J1833-0827, and support the possible associations W41/PSR J1833-0827 also. However, the pulsar is about $20'$ away from the extended γ -ray source and is not associated with HESS J1834-087.

TWW and LDA acknowledge support from the Natural Sciences and Engineering Research Council of Canada. The research at UMass is supported by the NASA/CXC under the grant GO5-6057X. TWW thanks support from the Natural Science Foundation of China. We thank Dr. Stil for providing the VGPS data. This publication makes use of molecular line data from the Boston University-FCRAO Galactic Ring Survey (GRS). The NRAO is a facility of the National Science Foundation operated under cooperative agreement by Associated Universities, Inc.

REFERENCES

- Aharonian, F., Akhperjanian, A.G., Bazer-Bachi, A.R. et al., 2006, ApJ, 636, 777
 Aharonian, F., Akhperjanian, A.G., Bazer-Bachi, A.R. et al. 2005a, A&A, 437, L7
 Aharonian, F., Akhperjanian, A.G., Aye, K.-M. et al. 2005b, Science, 307, 1938
 Albert, J., Aliu, E., Anderhub, H. et al. 2006, ApJ, 643, L53
 Cox, D., 1972, ApJ, 178, 159
 Dame, T.M., Hartmann, D., Thaddeus, P., 2001, ApJ, 547, 792
 Dame, T.M., Elmegreen, B.G., Cohen, R.S. et al., 1986, ApJ, 305, 892
 Enomoto R., Tanimori, T., Naito, T. 2002, Nature, 416, 823 2004, MNRAS, 353, 1311
 Landi, R., Bassani, L., Malizia, A., 2006, ApJ, 651, 190
 Langer, W.D., Penzias, A.A., 1990, ApJ, 357, 477
 Gaensler B.M. & Johnston, S., 1995, MNRAS, 275, 73
 Kassim, N.E., 1992, AJ, 103, 943
 Jackson, J.M., Rathborne, J.M., Shah, R.H. et al. 2006, ApJ Suppl., 163, 145
 Malkov E., Drury L.O'C., 2001, Rep. Prog. Phys., 64, 429
 Taylor, J.H., Manchester, R.N. & Lyne, A.G., 1993, ApJS, 88, 529.
 Torres, D.F., Romero, G.E., Dame, T.M. et al. 2003, Phy. Reports, 382, 303
 Stil, J.M., Taylor, A.R., Dickey, J.M. et al. 2006, AJ, 132, 1158
 Wang Q.D., 2004, ApJ, 612, 159
 Weekes, T.C., Cawley, M.F., Fegan, D.J. et al., 1989, ApJ, 342, 379
 Weisberg J.M., Siegel, M.H., Frail, D.A. et al., 1995, 447, 204
 Yamazaki, R., Kohri, K., Bamba, A. et al. 2006, MNRAS, 371, 1975